Mechanism of Radiation Damage Reduction in Equiatomic Multicomponent Single Phase Alloys

F. Granberg
Department of Physics, University of Helsinki, Post-office box 43, FIN-00014, Finland

K. Nordlund*
Department of Physics, University of Helsinki, Post-office box 43, FIN-00014, Finland

Mohammad W. Ullah
Department of Physics, University of Helsinki, Post-office box 43, FIN-00014, Finland and Materials Science and Technology Division, Oak Ridge National Laboratory, Oak Ridge, Tennessee 37831, USA

K. Jin
Materials Science and Technology Division, Oak Ridge National Laboratory, Oak Ridge, Tennessee 37831, USA

C. Lu
Department of Nuclear Engineering and Radiological Sciences, University of Michigan, Ann Arbor, Michigan 48109-2104, USA

H. Bei
Materials Science and Technology Division, Oak Ridge National Laboratory, Oak Ridge, Tennessee 37831, USA

L. M. Wang
Department of Nuclear Engineering and Radiological Sciences, University of Michigan, Ann Arbor, Michigan 48109-2104, USA

F. Djurabekova
Helsinki Institute of Physics, University of Helsinki, Post-office box 43, FIN-00014, Finland and Department of Physics, University of Helsinki, Post-office box 43, FIN-00014, Finland

W. J. Weber
Materials Science and Technology Division, Oak Ridge National Laboratory, Oak Ridge, Tennessee 37831, USA and Department of Materials Science and Engineering, University of Tennessee, Knoxville, Tennessee 37996, USA

Y. Zhang†
Materials Science and Technology Division, Oak Ridge National Laboratory, Oak Ridge, Tennessee 37831, USA

(Received 5 November 2015; published 1 April 2016)

Recently a new class of metal alloys, of single-phase multicomponent composition at roughly equal atomic concentrations ("equiatomic"), have been shown to exhibit promising mechanical, magnetic, and corrosion resistance properties, in particular, at high temperatures. These features make them potential candidates for components of next-generation nuclear reactors and other high-radiation environments that will involve high temperatures combined with corrosive environments and extreme radiation exposure. In spite of a wide range of recent studies of many important properties of these alloys, their radiation tolerance at high doses remains unexplored. In this work, a combination of experimental and modeling efforts reveals a substantial reduction of damage accumulation under prolonged irradiation in single-phase NiFe and NiCoCr alloys compared to elemental Ni. This effect is explained by reduced dislocation mobility, which leads to slower growth of large dislocation structures. Moreover, there is no observable phase separation, ordering, or amorphization, pointing to a high phase stability of this class of alloys.

DOI: 10.1103/PhysRevLett.116.135504

The accelerated development of new technologies for efficient energy production demands new materials that are tolerant to extreme environments and can operate reliably at high temperatures. Operating thermal power plants—whether conventional or nuclear—at higher temperatures

is, from a principal point of view, a simple way to increase energy efficiency, but requires, in practice, materials that can withstand the increased operation window. Many of the new energy production concepts considered, such as concentrated solar energy and several Generation-IV nuclear concepts, include components with flowing liquid salts or metals, posing serious corrosion challenges [1–3]. Both electric power generators and nuclear fusion power plants involve high magnetic fields [4], adding a further class of materials properties that needs to be considered. With respect to these requirements on the materials, a recently developed class of metal alloys shows high promise to exhibit greatly improved properties. Most traditional metal alloys involve one principal element alloyed by much lower concentrations of others, or mixtures of several different phases. Systematic synthesis and study of alloys with multiple elements at equal (called "equiatomic" [5] or, in case they contain at least 5 elements, "high-entropy" alloys) or roughly equal concentrations in a single phase structure has, however, started only recently [5,6]. Intense recent work has revealed that these alloys have the ability to maintain good mechanical properties both at cryogenic conditions [7] and up to very high temperatures (∼1000 °C), as well as a good corrosion resistance [8]. Hence, they are strong candidates to resolve many challenges imposed by extreme environments. However, in the particular case of nuclear reactors, there is the additional complication of radiation damage. In particular, realization of new Generation IV fission reactor concepts [9,10], that will have many improved features (e.g., the capability to burn used nuclear fuel), as well as tokamaklike fusion power plants [10,11], will both subject materials in the reactors to very high neutron irradiation loads. Hence, to realize the great potential of equiatomic and high-entropy alloys in nuclear environments, it is crucial to consider also radiation damage and its buildup in these materials. Recently, preliminary estimations of the possible reduction of radiation damage in Ni equiatomic alloys were done based on analysis of formation of point defects and initial damage structures [12]. Here we, in these multicomponent single phase alloys, focus on the issue of damage buildup and its mechanisms, crucial for practical applications.

Even though some classes of steels and other metal alloys are known to have high radiation tolerance, their properties do start to change immediately after the onset of irradiation [10,13]. This has motivated an intense ongoing search for new classes of materials with improved radiation hardness. New materials, shown to have high radiation tolerance include nanocrystalline materials [14–16], multilayered nanomaterials [17], and nanofoams [18,19]. Although all of these are promising for some applications, the high fraction of surface or interface, which are thermodynamically unstable, makes nanostructures in general unreliable for long operational times at elevated temperatures. For such conditions, typical for nuclear reactors, it is very valuable to find homogeneous and stable materials with improved radiation tolerance, and equiatomic or high-entropy alloys could become such a class of materials.

In this Letter, we examine the radiation tolerance of single-phase equiatomic alloys of two and three components: NiFe and NiCoCr, by experiments and molecular dynamics computer simulations, with particular emphasis on the damage buildup effects. The materials are not chosen for any specific application in mind, but to investigate the radiation hardness of equiatomic alloys in general. We show that the multielemental composition of the equiatomic materials slows down dislocation motion in them, leading to a strong (factor of ∼2–3) reduction in radiation damage. Understanding of the actual mechanisms of reduction of radiation damage in the equiatomic metal alloys will allow for a focused search of other combinations of alloying metals with even more improved radiation tolerance.

For our study, we chose the NiFe and NiCoCr alloys since they could be synthesized experimentally as high-quality single crystals [20], while maintaining a completely random atom arrangement within a well-defined face-centered cubic (fcc) crystal. (see methods section in the Supplemental Material [21]). Moreover, interatomic potentials for the same alloy composition were readily available [22–24]. We investigated the radiation response in these materials in comparison to pure Ni, which has the same crystal structure. We emphasize that the outcome of radiation in these materials is by no means *a priori* clear: while in elemental metals the damage levels saturate at a relatively low defect concentration, around 1% [25], some metal alloys are known to amorphize under irradiation [26], indicating a major increase in damage production.

The experimental pure Ni and equiatomic alloy samples were irradiated with Ni and Au ions with the energies 1.5 and 3 MeV, respectively, producing damage in the dense cascades similar to those produced by neutron recoils in nuclear reactors [25]. The damage was analyzed by Rutherford backscattering and channeling (RBS/C; see methods section in the Supplemental Material [21]). The results in Fig. 1 show that there is a major (a factor 2–3) reduction in the damage in the NiFe and NiCoCr equiatomic alloys, as compared to the pure element Ni. Moreover, the three elemental NiCoCr alloy shows a still lower damage level than the two elemental NiFe.

Our cross-sectional transmission electron microscopy (TEM) analysis (Figs. 2 and 3) of Ni and NiFe irradiated by 3 MeV Au ions to 2×10^{13} and 1×10^{14} ions/cm^2 at room temperature shows that the depth distribution of defect clusters strongly depends on the ion fluence and the composition of the material. As expected from previous works showing that dislocations have a crucial role in irradiated metals [27–32], we observe typical features of

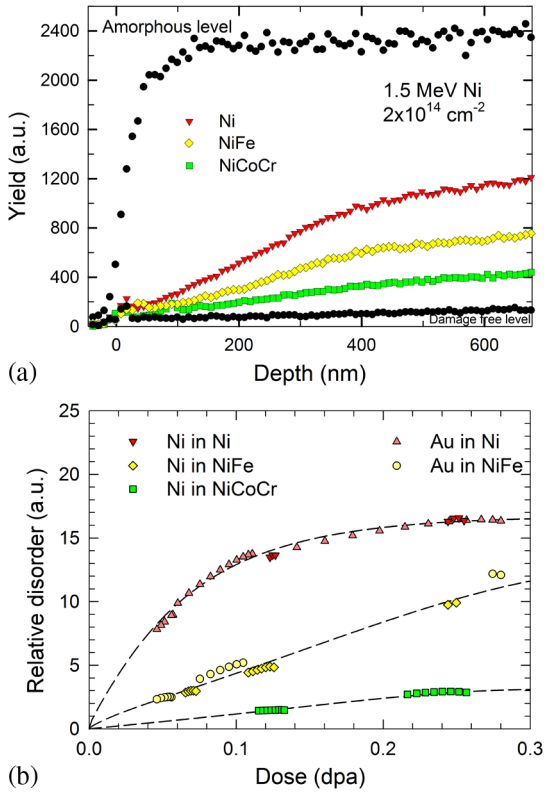

FIG. 1. Comparison of irradiation-induced damage in elemental Ni and equiatomic alloys. (a) Rutherford backscattering spectra showing different irradiation response. The higher damage level is observed in the order of Ni, NiFe, and NiCoCr after 1.5 MeV Ni to a fluence of 2×10^{14} cm^{-2}. (b) Relative disorder in the model systems investigated under 1.5 MeV Ni and 3 MeV Au irradiations. While there exists large uncertainty (~20%) due to the SRIM predictions and channeling analysis, the data clearly show that under these irradiation conditions, much less damage is produced in the NiFe and NiCoCr equiatomic alloys. The dashed lines are curve fits to the data to guide the eye.

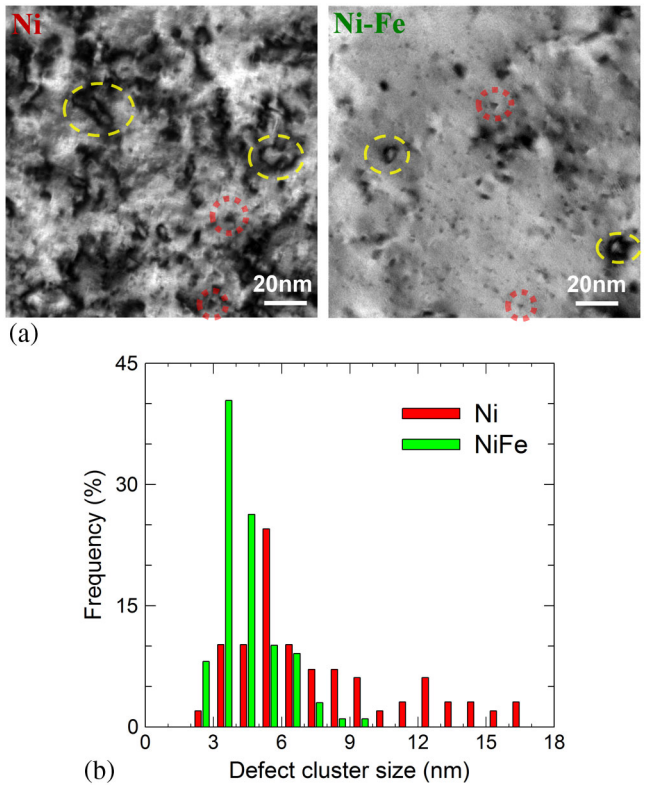

FIG. 2. Defect cluster distributions in Ni and NiFe at low fluence. (a) High magnification bright-field images of Ni and NiFe samples irradiated using 3 MeV Au ions to a fluence of 2×10^{13} cm^{-2} (Peak dose at 155 nm is ~0.1 dpa) under two beam conditions, $g = [200]$, and (b) size distribution of defect clusters. Interstitial-type dislocation loops are indicated by the dashed circles, and small triangles marked by the dotted circles are characterized as SFT. The scale bar is 20 nm.

dislocation loops and vacancy-type stacking fault tetrahedra (SFT) in all investigated samples. However, comparison of the NiFe micrographs with the Ni ones shows clearly that there is less damage in NiFe, and the feature sizes are smaller. This is confirmed by quantitative comparison of the defect cluster sizes [Figs. 2(b) and 3(b)]. Moreover, no signs of phase separation or ordering is observed even at the highest doses studied. No cracking was observed in the samples, which gives promise that there is no drastic reduction of ductility under irradiation. Systematic studies of the mechanical property change after irradiation are in progress.

To establish the origin of the damage reduction and reason for a strong dislocation signal, we turn to molecular dynamics (MD) computer simulations, a method widely used to examine radiation damage production in metals [27,33,34] (see methods section in the Supplemental Material [21]). We carried out simulations of radiation collision cascades consecutively in the same simulation cell to reach the high doses of about 0.57 displacements per atom (dpa [35]) that can be compared with the experiments. The simulations were carried out by running 1500–1800 recoils at a typical subcascade energy of 5 keV in a segment of material far from the surface, to mimic damage production at the experimental depths of hundreds of nanometers.

The MD results of damage production under prolonged irradiation show three results of direct relevance to interpret the experiments. First, the point defect damage level saturates with a dose at about 0.3 dpa, consistent with previous experiments in elemental metals [25]. The results up to the same dose as in the experiments [see Fig. 4(a)] demonstrate, in agreement with the TEM and RBS measurements, that equiatomic alloys are well resistant to amorphization and do not show any signs of separation or ordering. Second, the defect clustering analysis showed that after the cascade damage started to overlap with preexisting defects, recombination effects [36,37] tended to remove point defects, while defect clusters grew in size and started to form ordered defect structures known as (partial and perfect) dislocation loops. These can be

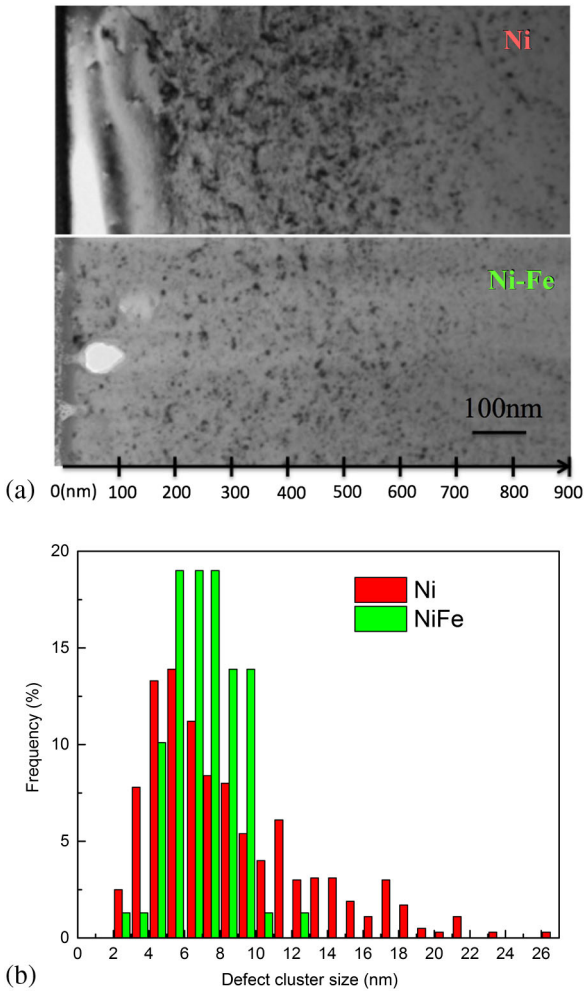

FIG. 3. Defect cluster distributions in Ni and NiFe at high fluence. Bright-field cross-sectional TEM images ($g = [200]$) showing the overall irradiated region in Ni and NiFe (a) samples after 3 MeV Au ion irradiation to 1×10^{14} cm^{-2} (Damage peak at 155 nm is equivalent to 0.57 dpa). (b) Size distribution of defect clusters.

visually seen Fig. 4(c), and their growth and interactions are illustrated in the movies in the Supplemental Material [21]. Third, the analysis of damage distribution in clusters showed that the crucial difference between NiFe and NiCoCr compared to Ni is that in the alloys, the fraction of damage in large clusters is smaller [Fig. 4(b)]. Since the TEM method cannot detect the small defect clusters most prevalent in the simulation cells of a limited size, a one-to-one comparison of experimental and simulation cluster size distributions is not feasible in the current work. However, because TEM detects the large defect formations, this simulation result on large defect clusters is the most suitable for comparison with the experiments.

The reduced fraction of damage in the large ($\geq$10 defects) dislocation structures was observed with two different MD interatomic potentials used (see methods section in the Supplemental Material [21]), and is fully consistent with the experimental observations on the differences between the materials. The diameter of the defects are also smaller in the alloys than in pure Ni, see Fig. 4(b) inset, and have a similar size distribution peaked stronger at small cluster sizes for the alloys NiFe and NiCoCr. Thus, we conclude that the reason for the damage reduction in the equiatomic alloys studied here [Fig. 4(a)] is that the dislocation structures are in these materials smaller than in the elemental material.

To determine the mechanism by which the dislocation structures observed in the simulations are smaller in NiFe and NiCoCr compared to Ni, we separately analyzed the mobility of edge dislocations in these materials, following the approach in Ref. [38]. Lattice distortions caused by the different atomic types in equiatomic alloys can be expected to affect the dislocation mobility in these materials. We found that the edge dislocation in NiCoCr is indeed less mobile than that in NiFe, which in turn is less mobile than that in Ni. The difference in dislocation mobility in the alloys and pure Ni depended on the strain rate used, but was clearly at least a factor of 2. The onset stress for movement is also much higher for the alloys compared with that in the pure element. Hence, we conclude that distortion of the crystal lattice structure in the equiatomic alloying materials is able to hinder the dislocation movement, resulting in smaller damage structures in NiFe and NiCoCr, making them also less likely to grow. This deduction is further supported by the movies provided in the Supplemental Material [21], which show visually that the damage evolution involves extensive discontinuous motion of different dislocation structures, all induced by the radiation condition. The velocity v of a dislocation, once it becomes mobile, depends on an external macroscopic stress σ as [39]

$$v = M_d b \sigma, \tag{1}$$

where M_d is the dislocation mobility constant and b the Burgers vector of the dislocation. Our results show that the mobility of dislocations in equiatomic alloys, M_d^{ea} are smaller than those in pure elements M_d^{el}. Because permanent deformation of metals is driven by dislocation motion $\propto v$ in metals, Eq. (1) implies that equiatomic alloys can be expected to be able to withstand higher macroscopic stresses σ than the corresponding pure elements. Moreover, we also compared our results qualitatively with similar runs carried out in widely used ferritic Fe-Cr alloys [3,10]. In spite of different lattice structures, we observe a similar relative damage reduction compared to the pure element, but find that it is larger in the equiatomic alloys (see Supplemental Material [21]).

We note that the simulated dose rate is orders of magnitude higher than the experimental one due to the limited time scale available for conventional MD simulations. In particular, at experimental dose rates, there would be much more time for point defects to move

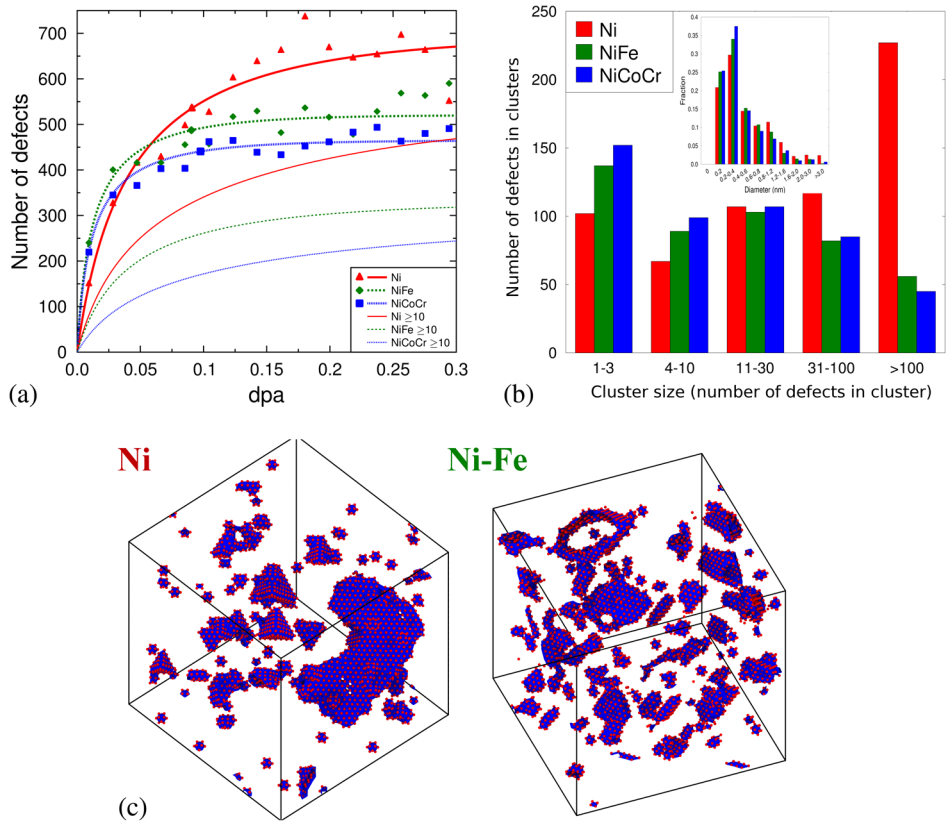

FIG. 4. Molecular dynamics results of damage production in Ni, NiFe, and NiCoCr. (a) Buildup of total number of defects and number of defects in clusters larger or equal to 10, divided into point defects and defect clusters. The lines are fits of a function to the data points to guide the eye. The individual data points show fairly large fluctuations since individual dislocation recombination reactions (see text) can cause large changes in the defect numbers. (b) Average cluster size distribution at the dose from ~0.4 dpa to the end. The inset shows the same distribution grouped by cluster diameter. (c) Defect structures in Ni and NiFe at a dose of 0.5 dpa. The atoms shown are filtered by removing the perfect structured fcc atoms according to an adaptive common neighbor analysis, to show only atoms that are part of a defective structure.

between the subcascade events. However, most of the point defects would be absorbed by the dislocations, and hence the effect of practically all defects being in damage clusters would be achieved at even lower doses than in the simulations. Hence the main conclusion of the difference in damage production at higher doses ($\gtrsim$0.1 dpa) being due to different dislocation sizes and mobility is not affected by the underestimation of point defect migration in the MD simulations.

To summarize, our combined experimental and simulation results show consistently that equiatomic metal alloys may be more resistant to radiation damage than the corresponding pure elements. Moreover, our analysis of the underlying mechanism of different equiatomic alloys establishes that alloy effects on significant reduction of dislocation mobility is generic and not specific to the current choice of materials or number of elements in the system. Further study is needed to establish whether additional damage reduction is possible with increasing number of elements and to find combinations of alloy composition and materials processing routes that would enable minimizing damage evolution in an engineering material at reasonable cost. Moreover, in nuclear fusion systems, the elements Co and Ni used in the currently studied equiatomic metal alloys would be needed to be replaced, to find alloys without elements that exhibit high activation under neutron irradiation. However, the difference between the NiFe and NiCoCr results already shows that a reduction will depend on material choice, and suggests that there may be alloys with even larger damage reduction than the currently observed one—especially in more chemically disordered alloys with increasing number of principal elements at significant concentrations (not necessarily at equiatomic concentrations), where the number of possible element combinations and alloy compositions are practically limitless.

This work was partially funded by the Academy of Finland SIRDAME project, and partially supported as part of the Energy Dissipation to Defect Evolution (EDDE), an Energy Frontier Research Center funded by the U.S. Department of Energy, Office of Science, Basic Energy Sciences. This work in part has been carried out by

F. G., K. N., and F. D. within the framework of the EUROfusion Consortium and has received funding from the Euratom research and training programme under Grant Agreement No. 633053. The views and opinions expressed herein do not necessarily reflect those of the European Commission. Grants of computer time from the Center for Scientific Computing in Espoo, Finland, are gratefully acknowledged. Ion beam work was performed at the University of Tennessee-Oak Ridge National Laboratory Ion Beam Materials Laboratory (IBML) located at the campus of the University of Tennessee, Knoxville. Part of the simulation used resources of the National Energy Research Scientific Computing Center, supported by the Office of Science, U.S. Department of Energy, under Contract No. DEAC02-05CH11231. This manuscript has been authored by UT-Battelle, LLC under Contract No. DE-AC05-00OR22725 with the U.S. Department of Energy. The United States Government retains and the publisher, by accepting the article for publication, acknowledges that the United States Government retains a nonexclusive, paid-up, irrevocable, world-wide license to publish or reproduce the published form of this manuscript, or allow others to do so, for United States Government purposes.

*Corresponding author.
kai.nordlund@helsinki.fi
†Corresponding author.
Zhangy1@ornl.gov

[1] R. I. Dunn, P. J. Hearps, and M. N. Wright, Molten-salt power towers: Newly commercial concentrating solar storage, Proc. IEEE **100**, 504 (2012).
[2] C. Singer, R. Buck, R. Pitz-Paal, and H. Mueller-Steinhagen, Economic potential of innovative receiver concepts with different solar field configurations for supercritical steam cycles, J. Sol. Energy Eng. **136**, 021009 (2013).
[3] K. L. Murty and I. Charit, Structural materials for gen-iv nuclear reactors: Challenges and opportunities, J. Nucl. Mater. **383**, 189 (2008).
[4] N. V. Khartchenko and V. M. Kharchenko, *Advanced Energy Systems*, 2nd ed. (CRC Press, Boca Raton, 2014).
[5] B. Cantor, I. T. H. Chang, P. Knight, and A. J. B. Vincent, Microstructural development in equiatomic multicomponent alloys, Mater. Sci. Eng. A **375–377**, 213 (2004).
[6] J.-W. Yeh, S.-K. Chen, S.-J. Lin, J.-Y. Gan, T.-S. Chin, T.-T. Shun, C.-H. Tsau, and S.-Y. Chang, Nanostructured high-entropy alloys with multiple principal elements: Novel alloy design concepts and outcomes, Adv. Eng. Mater. **6**, 299 (2004).
[7] B. Gludovatz, A. Hohenwarter, D. Catoor, E. H. Chang, E. P. George, and R. O. Ritchie, A fracture-resistant high-entropy alloy for cryogenic applications, Science **345**, 1153 (2014).
[8] M.-H. Tsai and J.-W. Yeh, High-entropy alloys: A critical review, Mater. Res. Lett. **2**, 107 (2014).
[9] L. K. Mansur, A. F. Rowcliffe, R. K. Nanstad, S. J. Zinkle, W. R. Corwin, and R. E. Stoller, Materials needs for fusion, generation iv fission reactors and spallation neutron sources—similarities and differences, J. Nucl. Mater. **329–333**, 166 (2004).
[10] S. J. Zinkle and J. T. Busby, Structural materials for fission & fusion energy, Mater. Today **12**, 12 (2009).
[11] A. Moslang, E. Diegele, M. Klimiankou, R. Lasser, R. Lindau, E. Lucon, E. Materna-Morris, C. Petersen, R. Pippan, J. W. Rensman, M. Rieth, B. van der Schaaf, H. C. Schneider, and F. Tavassoli, Towards reduced activation structural materials data for fusion demo reactors, Nucl. Fusion **45**, 649 (2005).
[12] Y. Zhang, G. Malcolm Stocks, K. Jin, C. Lu, H. Bei, B. C. Sales, L. Wang, L. K. Beland, R. E. Stoller, G. D. Samolyuk, M. Caro, A. Caro, and W. J. Weber, Influence of chemical disorder on energy dissipation and defect evolution in concentrated solid solution alloys, Nat. Commun. **6**, 8735 (2015).
[13] S. J. Zinkle, A. Möslang, T. Muroga, and H. Tanigawa, Multimodal options for materials research to advance the basis for fusion energy in the iter era, Nucl. Fusion **53**, 104024 (2013).
[14] Y. Zhang, M. Ishimaru, T. Varga, T. Oda, C. Hardiman, H. Xue, Y. Katoh, S. Shannon, and W. J. Weber, Nanoscale engineering of radiation tolerant silicon carbide, Phys. Chem. Chem Phys. **14**, 13429 (2012).
[15] H. Van Swygenhoven, P. M. Derlet, and A. G. Froseth, Stacking fault energies and slip in nanocrystalline metals, Nat. Mater. **3**, 399 (2004).
[16] A. R. Kilmametov, D. V. Gunderov, R. Z. Valiev, A. G. Balogh, and H. Hahn, Enhanced ion irradiation resistance of bulk nanocrystalline tini alloy, Scr. Mater. **59**, 1027 (2008).
[17] I. J. Beyerlein, A. Caro, M. J. Demkowicz, N. A. Mara, A. Misra, and B. P. Uberuaga, Radiation damage tolerant nanomaterials, Mater. Today **16**, 443 (2013).
[18] E. M. Bringa, J. D. Monk, A. Caro, A. Misra, L. Zepeda-Ruiz, M. Duchaineau, F. Abraham, M. Nastasi, S. T. Picraux, Y. Q. Wang, and D. Farkas, Are nanoporous materials radiation resistant?, Nano Lett. **12**, 3351 (2012).
[19] C. Anders, E. M. Bringa, and H. M. Urbassek, Sputtering of a metal nanofoam by Au ions, Nucl. Instrum. Methods Phys. Res., Sect. B **342**, 234 (2015).
[20] Z. Wu, Y. F. Gao, and H. Bei, Single crystal plastic behavior of a single-phase, face-center-cubic-structured, equiatomic fenicrco alloy, Scr. Mater. **109**, 108 (2015).
[21] See Supplemental Material at http://link.aps.org/supplemental/10.1103/PhysRevLett.116.135504 for additional technical details on the simulation and experimental method, as well as supplementary movies and a description of them.
[22] X. W. Zhou, R. A. Johnson, and H. N. G. Wadley, Misfit-energy-increasing dislocations in vapor-deposited cofeÕnife multilayers, Phys. Rev. B **69**, 144113 (2004).
[23] Z. Lin, R. A. Johnson, and L. V. Zhigilei, Computational study of the generation of crystal defects in a bcc metal target irradiated by short laser pulses, Phys. Rev. B **77**, 214108 (2008).

[24] G. Bonny, N. Castin, and D. Terentyev, Interatomic potential for studying ageing under irradiation in stainless steels: The fenicr model alloy, Model. Simul. Mater. Sci. Eng. **21**, 085004 (2013).
[25] R. S. Averback, R. Benedek, and K. L. Merkle, Ion-irradiation studies of the damage function of copper and silver, Phys. Rev. B **18**, 4156 (1978).
[26] N. Karpe, K. K. Larsen, and J. Bottiger, Phase formation induced by ion irradiation and electrical resistivity of aluminum-transition-metal alloys, Phys. Rev. B **46**, 2686 (1992).
[27] K. Nordlund, J. Keinonen, M. Ghaly, and R. S. Averback, Coherent displacement of atoms during ion irradiation, Nature (London) **398**, 49 (1999).
[28] K. Nordlund and F. Gao, Formation of stacking fault tetrahedra in collision cascades, Appl. Phys. Lett. **74**, 2720 (1999).
[29] T. Diaz de la Rubia, H. M. Zbib, T. A. Khraishi, B. D. Wirth, M. Victoria, and M. J. Caturla, Multiscale modelling of plastic flow localization in irradiated materials, Nature (London) **406**, 871 (2000).
[30] K. Arakawa, K. Ono, M. Isshiki, K. Mimura, M. Uchikoshi, and H. Mor, Observation of the one-dimensional diffusion of nanometer-sized dislocation loops, Science **318**, 956 (2007).
[31] Y. Matsukawa and S. J. Zinkle, One-dimensional fast migration of vacancy clusters in metals, Science **318**, 959 (2007).
[32] L. Sun, A. V. Krasheninnikov, T. Ahlgren, K. Nordlund, and F. Banhart, Plastic Deformation of Single Nanometer-Sized Crystals, Phys. Rev. Lett. **101**, 156101 (2008); see also commentary on article by S. Suresh and J. Li, Materials science: Deformation of the ultra-strong, Nature (London) **456**, 716 (2008).
[33] K. Nordlund, M. Ghaly, R. S. Averback, M. Caturla, T. Diaz de la Rubia, and J. Tarus, Defect production in collision cascades in elemental semiconductors and fcc metals, Phys. Rev. B **57**, 7556 (1998).
[34] R. S. Averback and T. Diaz de la Rubia, Displacement damage in irradiated metals and semiconductors, in *Solid State Physics*, edited by H. Ehrenfest and F. Spaepen (Academic Press, New York, 1998), Vol. 51, p. 281.
[35] K. Nordlund, S. J. Zinkle, T. Suzudo, R. S. Averback, A. Meinander, F. Granberg, L. Malerba, R. Stoller, F. Banhart, B. Weber, F. Willaime, S. Dudarev, and D. Simeone, OECD Nuclear Energy Agency, Report No. NEA/NSC/DOC (2015)9, 2015.
[36] K. Nordlund and R. S. Averback, Point defect movement and annealing in collision cascades, Phys. Rev. B **56**, 2421 (1997).
[37] F. Gao, D. J. Bacon, A. F. Calder, P. E. J. Flewitt, and T. A. Lewis, Computer simulation study of cascade overlap effects in alpha-iron, J. Nucl. Mater. **230**, 47 (1996).
[38] Yu. N. Osetsky and D. J. Bacon, An atomic-level model for studying the dynamics of edge dislocations in metals, Model. Simul. Mater. Sci. Eng. **11**, 427 (2003).
[39] J. P. Hirth and J. Lothe, *Theory of Dislocations*, 2nd ed. (Krieger, Malabar, Florida, 1992).
[40] See Supplemental Material http://link.aps.org/supplemental/10.1103/PhysRevLett.116.135504, which includes Refs. [40–61].
[41] Z. Wu, H. Bei, F. Otto, G. M. Pharra, and E. P. George, Recovery, recrystallization, grain growth and phase stability of a family of fcc-structured multi-component equiatomic solid solution alloys, Intermetallics **46**, 131 (2014).
[42] B. Predel, *Phase Equilibria, Crystallographic and Thermodynamic Data of Binary Alloys*, edited by O. Madelung, Landolt-Börnstein, New Series III, Vol. IV/5 (Springer, Berlin, 1992).
[43] M. C. Troparevsky, J. R. Morris, P. R. C. Kent, A. R. Lupini, and G. M. Stocks, Criteria for Predicting the Formation of Single-Phase High-Entropy Alloys, Phys. Rev. X **5**, 011041 (2015).
[44] H. Bei and E. George, Microstructures and mechanical properties of a directionally solidified nial–mo eutectic alloy, Acta Mater. **53**, 69 (2005).
[45] R. E. Stoller, M. B. Toloczko, G. S. Was, A. G. Certain, S. Dwaraknath, and F. A. Garner, On the use of srim for computing radiation damage exposure, Nucl. Instrum. Methods Phys. Res., Sect. B **310**, 75 (2013).
[46] J. F. Ziegler, J. P. Biersack, and U. Littmark, *The Stopping and Range of Ions in Matter* (Pergamon, New York, 1985).
[47] M. P. Allen and D. J. Tildesley, *Computer Simulation of Liquids* (Oxford University Press, Oxford, England, 1989).
[48] M. Ghaly, K. Nordlund, and R. S. Averback, Molecular dynamics investigations of surface damage produced by kev self-bombardment of solids, Philos. Mag. A **79**, 795 (1999).
[49] K. Nordlund, J. Keinonen, M. Ghaly, and R. S. Averback, Coherent displacement of atoms during ion irradiation, Nature (London) **398**, 49 (1999).
[50] C. Björkas and K. Nordlund, Comparative study of cascade damage in fe simulated with recent potentials, Nucl. Instrum. Methods Phys. Res., Sect. B **259**, 853 (2007).
[51] L. Malerba, M. C. Marinica, N. Anento, C. Björkas, H. Nguyen, C. Domain, F. Djurabekova, P. Olsson, K. Nordlund, A. Serra, D. Terentyev, F. Willaime, and C. S. Becquart, Comparison of empirical interatomic potentials for iron applied to radiation damage studies, J. Nucl. Mater. **406**, 19 (2010).
[52] K. Nordlund, Molecular dynamics simulation of ion ranges in the 1–100 kev energy range, Comput. Mater. Sci. **3**, 448 (1995).
[53] J. F. Ziegler, SRIM-2013 software package, available online at http://www.srim.org.
[54] H. J. C. Berendsen, J. P. M. Postma, W. F. van Gunsteren, A. DiNola, and J. R. Haak, Molecular dynamics with coupling to external bath, J. Chem. Phys. **81**, 3684 (1984).
[55] J. Nord, K. Nordlund, and J. Keinonen, Molecular dynamics simulation of ion-beam-amorphization of si, ge and gaas, Nucl. Instrum. Methods Phys. Res., Sect. B **193**, 294 (2002).
[56] M. Backman, F. Djurabekova, O. H. Pakarinen, K. Nordlund, L. L. Araujo, and M. C. Ridgway, Amorphization of ge and si nanocrystals embedded in amorphous sio2 by ion irradiation, Phys. Rev. B **80**, 144109 (2009).
[57] A. Stukowski, Structure identification methods for atomistic simulations of crystalline materials, Model. Simul. Mater. Sci. Eng. **20**, 045021 (2012).

[58] D. Terentyev, M. Klimenkov, and L. Malerba, Confinement of motion of interstitial clusters and dislocation loops in bcc fe-cr alloys, J. Nucl. Mater. **393**, 30 (2009).

[59] L. Malerba, G. Bonny, D. Terentyev, E. E. Zhurkin, M. Hou, K. Vörtler, and K. Nordlund, Microchemical effects in irradiated Fe-Cr alloys as revealed by atomistic simulation, J. Nucl. Mater. **442**, 486 (2013).

[60] P. Olsson, J. Wallenius, C. Domain, K. Nordlund, and L. Malerba, Two-band modeling of α-prime phase formation in Fe-Cr., Phys. Rev. B **72**, 214119 (2005); see also Erratum, **74**, 229906(E) (2006).

[61] K. Nordlund, PARCAS computer code (2010). The main principles of the molecular dynamics algorithms are presented in Refs. [33–48]. The adaptive time step and electronic stopping algorithms are the same as in Ref. [52].

Supplementary material to "Mechanism of Radiation Damage Reduction in Equiatomic Multicomponent Single Phase Alloys"

F. Granberg
Department of Physics, Post-office box 43, FIN-00014 University of Helsinki, Finland

K. Nordlund
*Department of Physics, Post-office box 43, FIN-00014 University of Helsinki, Finland**

Mohammad W. Ullah
Department of Physics, Post-office box 43, FIN-00014 University of Helsinki, Finland and
Materials Science and Technology Division, Oak Ridge National Laboratory, Oak Ridge, Tennessee 37831, USA

K. Jin
Materials Science and Technology Division, Oak Ridge National Laboratory, Oak Ridge, Tennessee 37831, USA

C. Lu
Department of Nuclear Engineering and Radiological Sciences,
University of Michigan, Ann Arbor, Michigan 48109-2104, USA

H. Bei
Materials Science and Technology Division, Oak Ridge National Laboratory, Oak Ridge, Tennessee 37831, USA

L. M. Wang
Department of Nuclear Engineering and Radiological Sciences,
University of Michigan, Ann Arbor, Michigan 48109-2104, USA

F. Djurabekova
Helsinki Institute of Physics, Post-office box 43, FIN-00014 University of Helsinki, Finland and
Department of Physics, Post-office box 43, FIN-00014 University of Helsinki, Finland

W. J. Weber
Materials Science and Technology Division, Oak Ridge National Laboratory, Oak Ridge, Tennessee 37831, USA and
Department of Materials Science and Engineering,
University of Tennessee, Knoxville, Tennessee 37996, USA

Y. Zhang
Materials Science and Technology Division, Oak Ridge National Laboratory, Oak Ridge, Tennessee 37831, USA†

(Dated: March 28, 2016)

SUPPLEMENTARY MOVIES

The supplementary material includes the two movie files

Ni-5kev-1500-recoils.mov

and

NiFe-5kev-1500-recoils.mov

These quicktime movies illustrate the buildup of damage in Ni and NiFe (see main Letter). The movies show a 2D projection of all atom positions in a cubic simulation cell that is 108 Å in each dimension. Each dot illustrates the position of an atom, with blue dots representing Ni and red dots Fe. Each frame shows the final atom positions after one irradiation cascade event. The irradiation dose is given in units of displacements-per-atom (dpa).

Since the cells are crystalline, atoms in the same perfect crystal row are all plotted on top of each other, and hence only the atoms at the top are visible. Atoms in interstitial defects and stacking faults are, however, visible at any depth since they are outside the perfect crystal rows.

The movies show how, after the first few irradiation events, small stacking faults (bounded by partial dislocation loops) form in the cells. On increasing dose, they grow when additional cascades form damage near them,

and part of this damage is absorbed by the preexisting defects. The dislocation structures are also made mobile by the lattice heating and distortion caused by additional irradiation, evident from the rapid motion of defective regions. At the highest doses, the damage level has saturated (compare Fig. 4 in main Letter).

Comparison of the Ni and NiFe movies show that the defect structures in NiFe tend to be smaller than those in Ni (cf. detailed discussion in main Letter).

DETAILS ON METHODS

Synthesis of equiatomic alloys.

Polycrystalline ingots of Ni metal and Ni-based equiatomic alloys were prepared using high-purity elemental metals (> 99.9% purity) by arc melting and drop casting into cylindrical copper molds. The phase stability and the formation of single phases were carefully examined and confirmed using X-ray diffraction and microstructure characterization techniques [1]. The phase diagram for the investigated alloys, showing their phase stability, can be found for Ni and NiFe in Ref. 2 and the theoretical prediction of the phase stability of NiCoCr in Ref. 3. Face-centered cubic crystal Ni and alloys were grown in an optical floating zone furnace from the polycrystalline drop-cast ingots under an Ar atmosphere [4]. The quality and orientation of all crystals were inspected using backscatter Laue diffraction, re-oriented and cut normal to the <100> directions. Disks with thickness of $\sim$ 1 mm were electrochemically polished to remove the damage layers of the machining in order to produce damage-free surfaces, essential for ion channeling measurements.

Ion irradiation.

Irradiation response at room temperature of Ni, NiFe and NiCoCr were investigated with 3 MeV Au ions to fluences of 2×10^{13}, 5×10^{13} and 1×10^{14} cm^{-2} and 1.5 MeV Ni ions to 6×10^{13}, 1×10^{14} and 2×10^{14} cm^{-2}. Raster beam was used to ensure a homogeneous irradiation. The irradiation-induced damage peak was located at $\sim$ 155 nm and 370 nm for the Au and Ni cases, respectively. These energies were chosen to produce damage within a few hundreds of nanometers from the sample surface, where the damaged region can be readily characterized by microstructural analysis and ion channeling measurements with good depth resolution, but deep enough to avoid complication from surface effects. Predictions of local dose in displacements per atom (dpa) [5] and ion stopping range in Ni were estimated using the Stopping and Range of Ions in Matter (SRIM) code [6] under option of quick calculation of damage with a displacement threshold energy of 40 eV. The measured density of 8.908 g cm^{-3} is used in the SRIM calculation for pure Ni.

Rutherford backscattering and ion channeling analysis.

Rutherford backscattering spectrometry technique along major channel directions is used to verify the crystal quality and also to determine lattice distortion. A parallel 3.5 MeV He$^+$ beam that was well aligned along the <001> crystal direction was employed in the measurements. Following the ion energy deposition by either energetic Au ions or Ni ions, in-situ channeling measurements were subsequently carried out with a Si detector located at a scattering angle of 155° relative to the incoming He beam to record the increase of the backscattering yield due to irradiation-induced damage.

Microstructural characterization.

The cross-sectional TEM samples were prepared using focused ion beam (FIB) lift-out techniques utilizing the FEI Helios 650 Nanolab Dualbeam workstation. FIB-induced damage and sample thinning were performed by Ga$^+$ beam initially with energy of 30 keV and a current of 2.5 nA to 30 pA at an incident angle of $\pm$1.5° and sequentially down to 5 keV at the angle of $\pm$7° for 5 min. A flash polishing was conducted to remove residual damage from sample preparation. Bright field imaging of the same samples was done in a JEM 3011 TEM operating at 300 kV. Images were taken at an exposure time of 2 seconds.

Simulations.

The collision cascades in metals were simulated by means of molecular dynamics [7, 8] using the fully parallel PARCAS code developed within the group in Finland and extensively used for studies of cascades previously [9, 10]. We used two different potentials to describe the interatomic interactions in NiFe and NiCoCr alloys to verify that there is no significant dependence of the results on the choice of the interatomic potential. To describe the Ni-Co-Cr system, we combined the multi-elemental potentials by Zhou *et al.* [11] for Ni-Co with the Cr potential in the same formalism developed by Lin *et al.* [12]. To describe the interactions between the different elements in this system, we used the mixing scheme proposed in [11] between all the elements Ni-Co-Cr. For Fe-Ni, we used both the Fe-Ni potential formed in the same Zhou *et al.* set of potentials [11], and the completely independently developed pair-specific Fe-Ni potential by Bonny *et al.* [13]. Neither of the used potentials ex-

plicitly accounts for magnetism. Nevertheless it is implicitely taken into account, for instance, in the fitting of the cohesive energy. This remark is important with respect to results on damage buildup in FeNi, which is a magnetic material. However, previous simulation results on damage production in Fe with an explicit magnetic potential showed no significant difference compared to non-magnetic potentials. [14, 15] This justifies the use of potentials, where the magnetism is only implicitly accounted for. Both the Fe-Ni potentials were found to give similar results with respect to the damage production, showing that the results are not specific to a certain interatomic potential.

All three elemental compositions, Ni, NiFe and NiCoCr were simulated up to the dose ~ 0.57 dpa by running 1500 consecutive 5 keV recoils. Each set of the 1500 recoils was repeated three different times for each system using different seed numbers in the random number generator and different initial random cells, to show that the obtained results are not due to stochastic anomalities.

We dealt with the high energy effects associated with collision cascades by employing well established simulation methods for irradiation effects, namely an adaptive time step algorithm [16], electronic stopping power [17] and the ZBL repulsive potential [6] smoothly joined to the equilibrium potentials to describe the short distance interactions [9].

We used simulation cells comprising about 110 000 atoms to ensure that the heat spikes induced by the 5 keV recoils were fully developed within the cell, and that the periodic boundary conditions (applied at the cell sides in all dimensions) did not affect the final results. The simulation cell is too small for the largest defect structures seen in experiments (can be larger than 10 nm) to be represented, but a separate simulation setup, in FeCr, on a three times larger system showed that the damage level saturates at similar doses and defect levels, indicating that the key results are not sensitive to the system size.

During the cascade simulations, we controlled the temperature only at the sides of the simulation cell by applying Berendsen temperature control [18] on the border atoms. After about 25 ps (of the simulated 30 ps), no visible change in the damage structure was observed any more and the entire cell had cooled down to the ambient temperature (300 K). This will, as mentioned in the Letter, yield a much higher dose rate than that used in the experiments. However, the previous studies with similar approaches to simulate the damage buildup in semiconductors have shown a good agreement with experiments, although there was a similarly large difference in the dose rates [19, 20]. We ensured the homogeneous irradiation of the simulation cell by shifting the entire cell prior to the subsequent recoil event by a vector of random length (between zero and the cell size) and in a random direction. After the shift, atoms that were outside the cell boundaries were returned inside via the periodic cell boundaries. We monitored the development of stress in the simulations, and found no significant buildup of stress during the prolonged irradiation. A separate simulation was performed where a step of pressure relaxation to 0 kbar between the recoil events was added. This simulation gave identical results within statistical fluctuations to those without the extra step of pressure control.

Defects were analyzed with the Wigner-Seitz cell method [9] as well as with the program OVITO [21] and an adaptive common neighbor analysis implemented in the program.

Comparison with ferritic alloys

Currently a leading candidate class of materials for high radiation environments are ferritic steels based on about 10% Cr in a body-centered cubic (Fe) matrix [22, 23], which have been shown to exhibit good radiation resistance, likely due to the Cr slowing down dislocation loop migration [24, 25]. Hence, even though the Fe-Cr crystal structure is different to the currently studied face-centered cubic systems, it is of some interest to qualitatively compare the current results to those in Fe-10%Cr alloys. Hence we ran a set of similar cumulative 5 keV simulations for this Fe-Cr system modelled with the Olsson *et al.* potential [26]. The results of the comparison, Fig. 1, show that reduction in irradiation damage is superior for the equiatomic alloys compared to iron and the Fe-Cr alloy. We emphasize that the numerical values should not be compared directly to each other, due to differences in the crystal structure, but the relative change difference between the pair of element vs. alloys gives a first indication that the damage reductions obtained in equiatomic alloys may be quite comparable, or even better, than those in long-developed Fe-Cr alloys. However, as for the final Fe-Cr based steels which have undergone decades of development, clearly more work will be needed also on testing and optimizing alloying element concentrations and microstructure for equiatomic alloys, before they are ready for use as engineering materials.

SOURCE CODE AND INPUTS

To enable reproduction of the results, the Supplementary material also includes the complete source code of the software used to carry out the simulations 'parcas' [27]. The code, its documentation, and sample inputs for

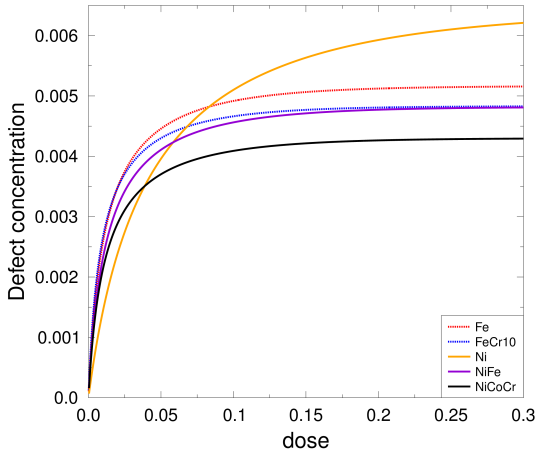

FIG. 1. Comparison of the results obtained for the equiatomic alloys compared with Fe and $Fe_{0.9}Cr_{0.1}$

Ni, NiFe and NiCoCr are provided as a `tar` archive package compressed in the `gzip` format. The package can be unpacked using the Linux/Unix command line command

```
tar xvfz parcas_source_code_inputs_package.tar.gz
```

The code can be compiled and run on any Linux/Unix distribution that carries, in addition to the standard system environment, an MPI Fortran compiler, following normal practises of Linux software compilation and execution. The file

```
README.INSTALL
```

provided in the main directory created by the unpacking contains installation and running instructions.

* kai.nordlund@helsinki.fi; Corresponding author
† Zhangy1@ornl.gov; Corresponding author

[1] Z. Wu, H. Bei, F. Otto, G. M. Pharra, and E. P. George, Intermetallics **46**, 131 (2014).
[2] B. Predel, *Phase Equilibria, Crystallographic and Thermodynamic Data of Binary Alloys*, edited by O. Madelung, Landolt-Börnstein, New Series III, Vol. IV/5 (Springer, Berlin, 1992).
[3] M. C. Troparevsky, J. R. Morris, P. R. C. Kent, A. R. Lupini, and G. M. Stocks, Phys. Rev. X **5**, 011041 (2015).
[4] H. Bei and E. George, Acta Materialia **53**, 69 (2005).
[5] R. Stoller, M. B. Toloczko, G. S. Was, A. G. Certain, S. Dwaraknath, and F. Garner, Nucl. Instr. Meth. Phys. Res. B **310**, 75 (2013).
[6] J. F. Ziegler, J. P. Biersack, and U. Littmark, *The Stopping and Range of Ions in Matter* (Pergamon, New York, 1985).
[7] M. P. Allen and D. J. Tildesley, *Computer Simulation of Liquids* (Oxford University Press, Oxford, England, 1989).
[8] M. Ghaly, K. Nordlund, and R. S. Averback, Phil. Mag. A **79**, 795 (1999).
[9] K. Nordlund, M. Ghaly, R. S. Averback, M. Caturla, T. Diaz de la Rubia, and J. Tarus, Phys. Rev. B **57**, 7556 (1998).
[10] K. Nordlund, J. Keinonen, M. Ghaly, and R. S. Averback, Nature **398**, 49 (1999).
[11] X. W. Zhou, R. A. Johnson, and H. N. G. Wadley, Phys. Rev. B **69**, 144113 (2004).
[12] Z. Lin, R. A. Johnson, and L. V. Zhigilei, Phys. Rev. B **77** (2008).
[13] G. Bonny, N. Castin, and D. Terentyev, Modelling Simul. Mater. Sci. Eng. **21**, 085004 (2013).
[14] C. Björkas and K. Nordlund, Nucl. Instr. Meth. Phys. Res. B **259**, 853 (2007).
[15] L. Malerba, M. C. Marinica, N. Anento, C. Björkas, H. Nguyen, C. Domain, F. Djurabekova, P. Olsson, K. Nordlund, A. Serra, D. Terentyev, F. Willaime, and C. Becquart, J. Nucl. Mater. **406**, 19 (2010).
[16] K. Nordlund, Comput. Mater. Sci. **3**, 448 (1995).
[17] J. F. Ziegler, SRIM-2013 software package, available online at *http://www.srim.org*.
[18] H. J. C. Berendsen, J. P. M. Postma, W. F. van Gunsteren, A. DiNola, and J. R. Haak, J. Chem. Phys. **81**, 3684 (1984).
[19] J. Nord, K. Nordlund, and J. Keinonen, Nucl. Instr. Meth. Phys. Res. B **193**, 294 (2002).
[20] M. Backman, F. Djurabekova, O. H. Pakarinen, K. Nordlund, L. L. Araujo, and M. C. Ridgway, Phys. Rev. B **80**, 144109 (2009).
[21] A. Stukowski, Modelling and Simulation in Materials Science and Engineering **20**, 045201 (2012).
[22] K. Murty and I. Charit, J. Nucl. Mater. **383**, 189 (2008).
[23] S. J. Zinkle and J. T. Busby, Materials Today **12**, 12 (2009).
[24] D. Terentyev, M. Klimenkov, and L. Malerba, J. Nucl. Mater. **393**, 30 (2009).
[25] L. Malerba, G. Bonny, D. Terentyev, E. E. Zhurkin, M. Hou, K. Vörtler, and K. Nordlund, J. Nucl. Mater. **442**, 486 (2013).
[26] P. Olsson, J. Wallenius, C. Domain, K. Nordlund, and L. Malerba, Phys. Rev. B **72**, 214119 (2005), see also Erratum, Phys. Rev. B 74, 229906 (2006).
[27] K. Nordlund, (2010), PARCAS computer code. The main principles of the molecular dynamics algorithms are presented in [8, 9]. The adaptive time step and electronic stopping algorithms are the same as in [16].